Supporting Information

Photochromism of neutral spiropyran in the crystalline state at room temperature

Zhen Wu, Qian Wang, Pengyu Li, Bing Fang, and Meizhen Yin*

State Key Laboratory of Chemical Resource Engineering, Beijing Advanced Innovation Center for Soft Matter Science and Engineering, Beijing Laboratory of Biomedical Materials, Beijing University of Chemical Technology, Beijing 100029 (P.R. China).

*E-mail: yinmz@mail.buct.edu.cn.

Syntheses

The synthesis routes of **SP-COOH** and **S1** are outlined below.

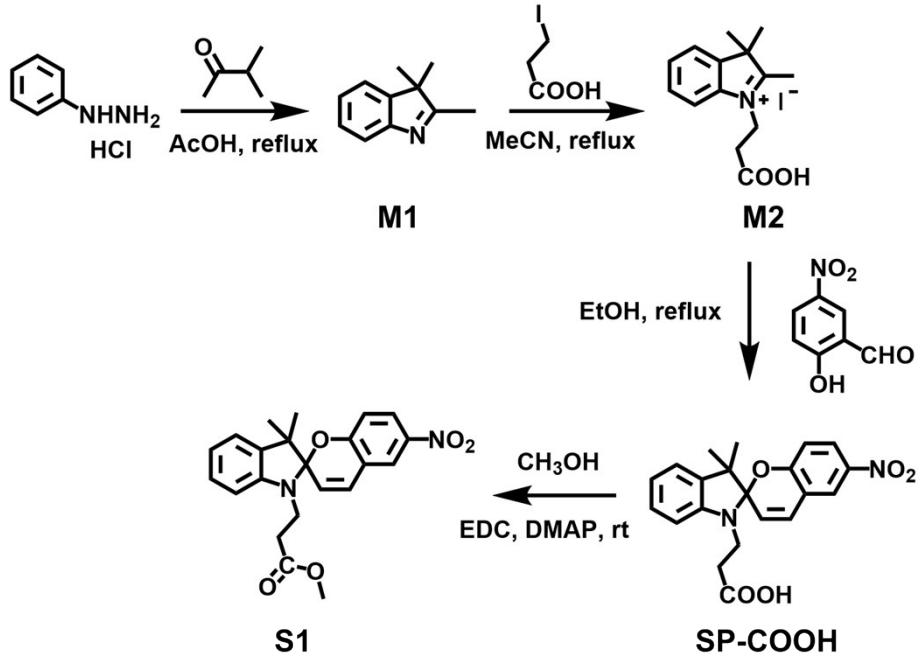

Scheme S1 Synthesis routes for the compounds of **SP-COOH** and **S1**.

2,3,3-trimethyl-3H-indole (M1): 3-methyl-2-butanone (1.6 mL, 15 mmol) was added

to a solution of phenylhydrazine hydrochloride (1.5 g, 10 mmol) in acetic acid (20 mL) in a round-bottomed flask fitted with a condenser and refluxed for 10 h, the solvent was removed under reduced pressure. The residue was extracted with dichloromethane and water to give **M1** as a brown oily liquid (1.2 g, yield 75%). ^{1}H NMR (400 MHz, DMSO) δ 7.47–7.35 (m, 2H), 7.26 (td, J = 7.5, 0.9 Hz, 1H), 7.17 (t, J = 7.4 Hz, 1H), 2.20 (s, 3H), 1.24–1.22 (m, 6H).

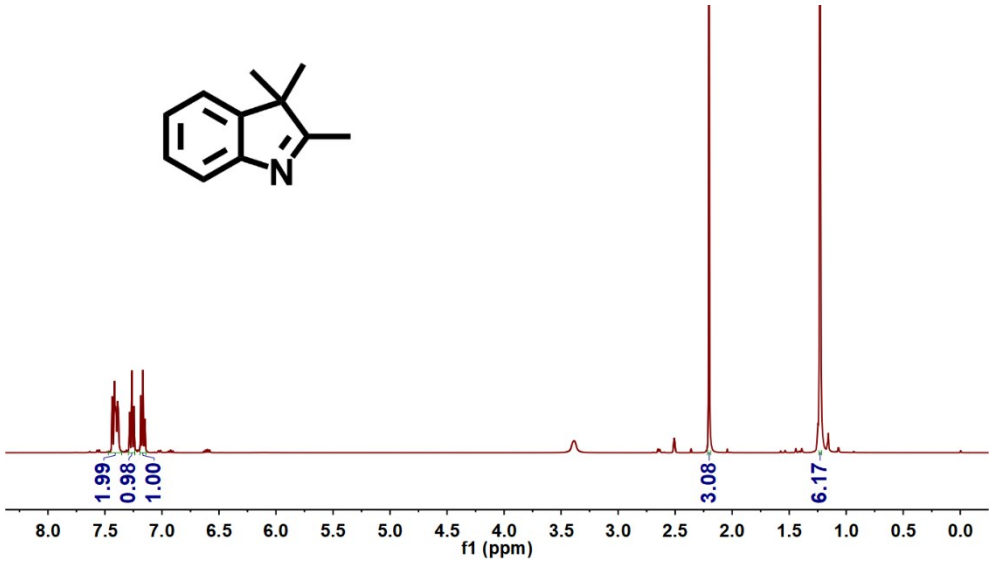

Fig. S1 ^{1}H NMR spectrum of compound **M1** in DMSO-d_6.

1-(2-carboxyethyl)-2,3,3-trimethyl-3H-indol-1-ium iodide (M2): **M1** (1 g, 6.3 mmol) and 3-iodopropanoic acid (1.3 g, 6.5 mmol) were dissolved in acetonitrile (15 mL) and refluxed for 8 h, then allowed to cool to room temperature. The solution was dispersed in diethyl ether and centrifuged to obtain the crude product. The crude was finally washed with diethyl ether and dried under reduced pressure to give **M2** as a pink solid (1.7 g, yield 75%). ^{1}H NMR (400 MHz, MeOD) δ 7.90 (dt, J = 7.4, 3.7 Hz, 1H), 7.78 (dt, J = 7.7, 3.8 Hz, 1H), 7.70–7.62 (m, 2H), 4.79 (t, J = 6.5 Hz, 2H), 3.10 (t, J = 6.5 Hz, 2H), 1.61 (s, 6H).

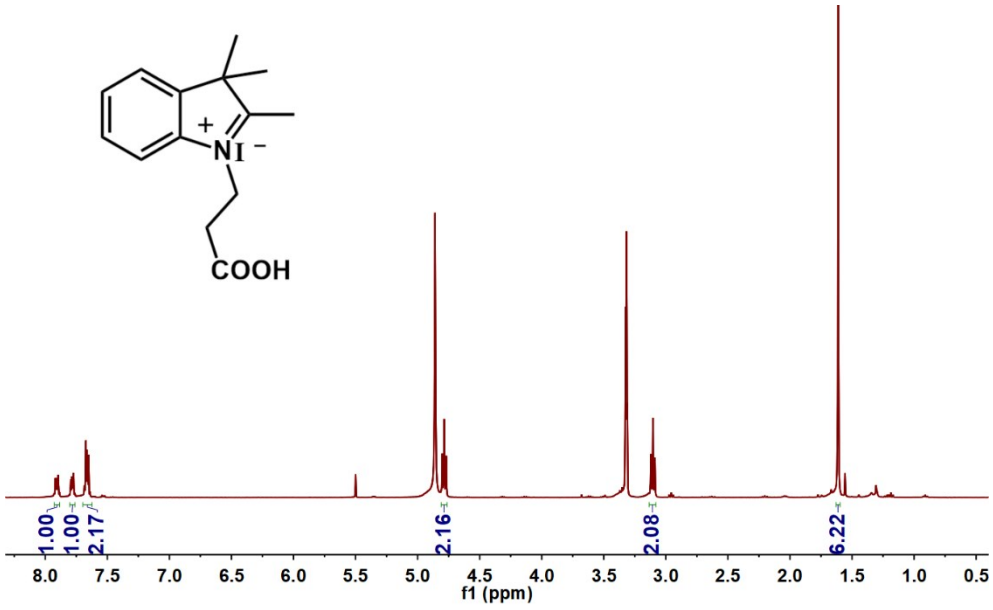

Fig. S2 ^{1}H NMR spectrum of compound **M2** in MeOD.

Compound SP-COOH: A solution of **M2** (502 mg, 1.4 mmol), 2-hydroxy-5-nitrobenzaldehyde (234 mg, 1.4 mmol), and pyridine (1.5 mL) in ethanol (15 mL) was refluxed under N_2 for 10 hours. After cooling to room temperature, the crude product is filtered and then washed three times with ethanol to obtain SP-COOH as a yellow solid (424 mg, yield 80%). ^{1}H NMR (400 MHz, DMSO) δ 12.21 (s, 1H), 8.22 (d, J = 2.6 Hz, 1H), 8.00 (dd, J = 9.0, 2.7 Hz, 1H), 7.21 (d, J = 10.4 Hz, 1H), 7.13 (t, J = 6.7 Hz, 2H), 6.87 (d, J = 9.0 Hz, 1H), 6.80 (t, J = 7.4 Hz, 1H), 6.67 (d, J = 7.9 Hz, 1H), 6.00 (d, J = 10.4 Hz, 1H), 3.55–3.36 (m, 2H), 2.62–2.53 (m, 1H), 2.47–2.39 (m, 1H), 1.19 (s, 3H), 1.08 (s, 3H). ESI-TOF: m/z calcd for $C_{21}H_{20}N_2O_5$, 380.14; found, 381.1451 ($M+H^+$). ^{1}H NMR, ^{13}C NMR and HR-MS (+) of compound **SP-COOH**:

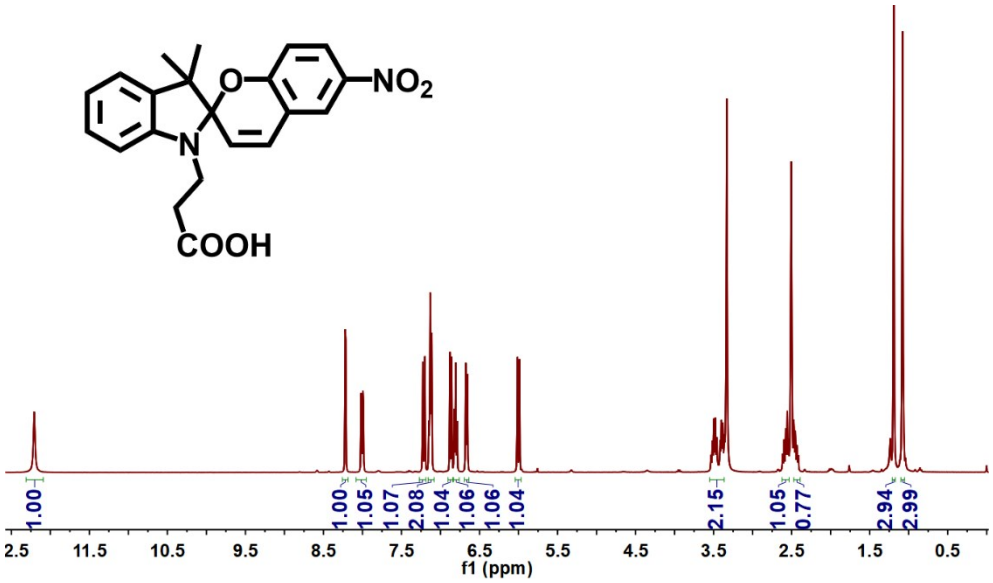

Fig. S3 ^{1}H NMR spectrum of compound **SP-COOH** in DMSO-d_6.

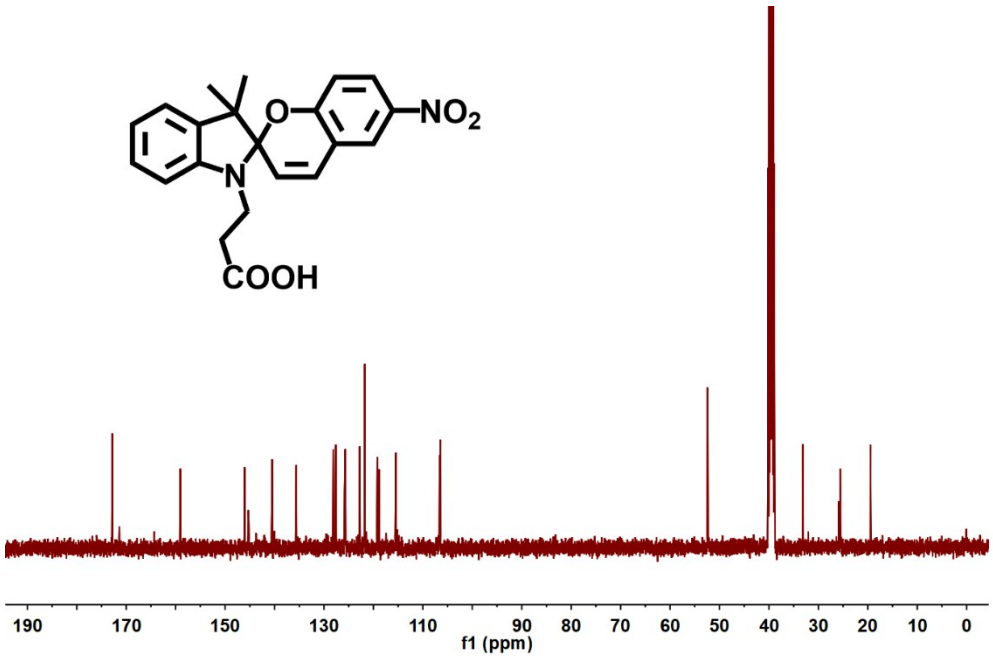

Fig. S4 ^{13}C NMR spectrum of compound **SP-COOH** in DMSO-d_6.

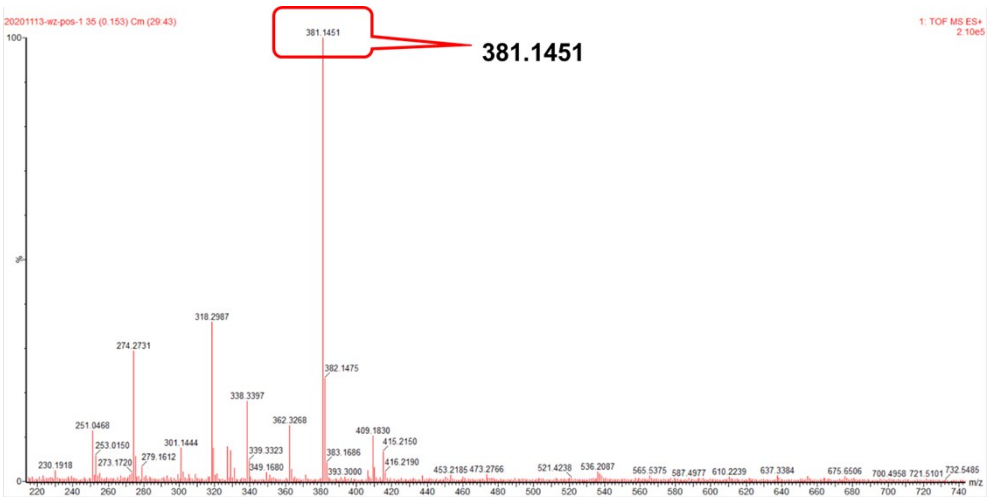

Fig. S5 ESI-MS spectrum of compound **SP-COOH**.

Compound S1: SP-COOH (225 mg, 0.59 mmol), EDC (252 mg, 0.64 mmol) and DMAP (20 mg, 0.16 mmol), were dissolved in 15 mL of anhydrous methanol under stirring at ambient temperature. After stirring for 24 h, the methanol solvent was removed under reduced pressure. The residues were chromatographically purified by DCM to obtain **S1** in a light yellow solid form (162 mg, yield 70%). ^{1}H NMR (400 MHz, $CDCl_3$) δ 8.04–7.97 (m, 2H), 7.20 (td, J = 7.7, 1.1 Hz, 1H), 7.12–7.05 (m, 1H), 6.90 (dd, J = 14.7, 8.7 Hz, 2H), 6.73 (d, J = 8.4 Hz, 1H), 6.61 (d, J = 7.8 Hz, 1H), 5.86 (d, J = 10.4 Hz, 1H), 3.69–3.46 (m, 5H), 2.75–2.50 (m, 2H), 1.26 (s, 3H), 1.15 (s, 3H) ESI-TOF: m/z calcd for $C_{22}H_{22}N_2O_5$, 394.15; found, 395.1619 ($M+H^+$). ^{1}H NMR, ^{13}C NMR and HR-MS (+) of compound **S1**:

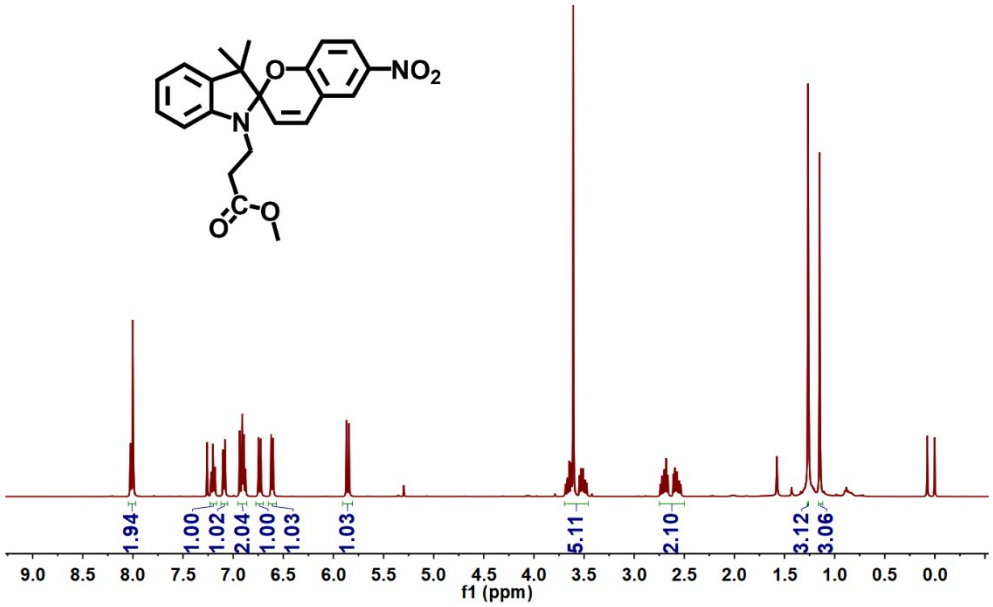

Fig. S6 ^{1}H NMR spectrum of compound **S1** in $CDCl_3$.

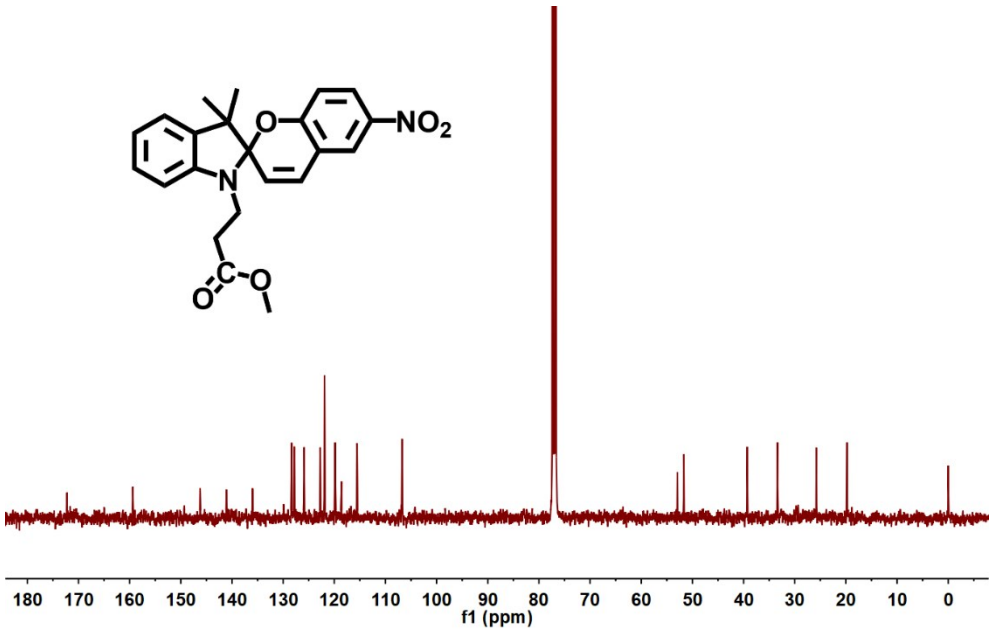

Fig. S7 ^{13}C NMR spectrum of compound **S1** in $CDCl_3$.

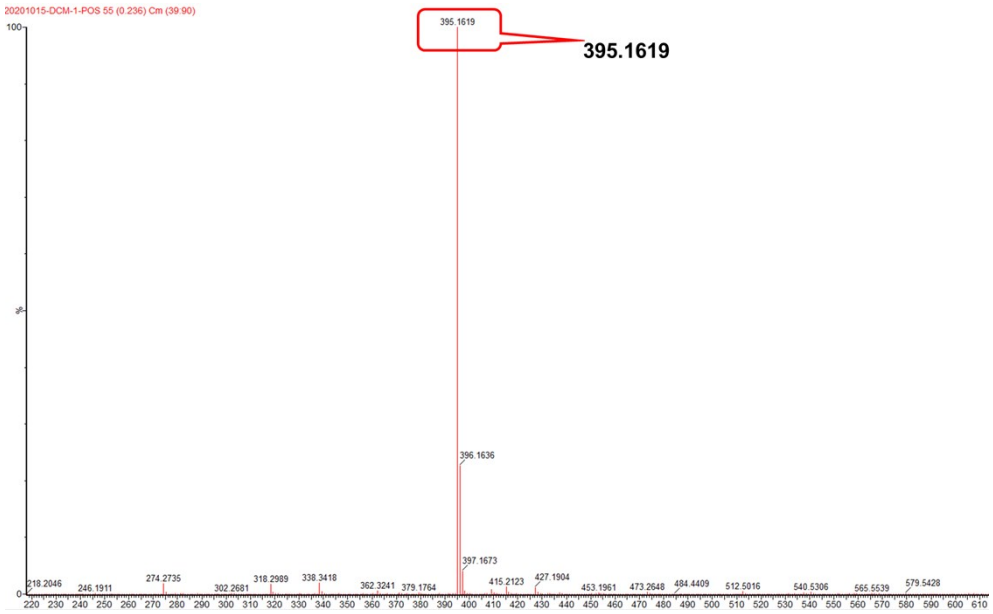

Fig. S8 ESI-MS spectrum of compound **S1**.

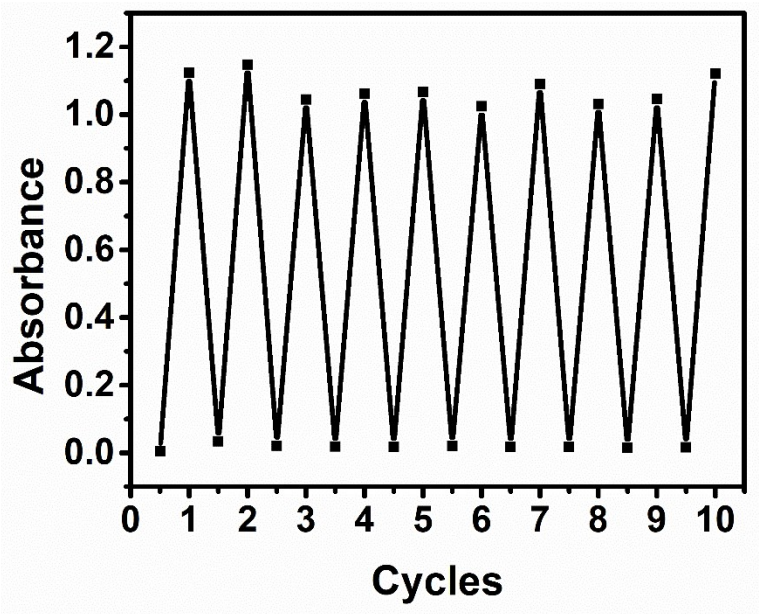

Fig. S9 Reversible switch of the absorption intensity of **S1** at 583 nm by alternating UV and visible light irradiation in DCM solution (concentration: 1×10^{-4} M).

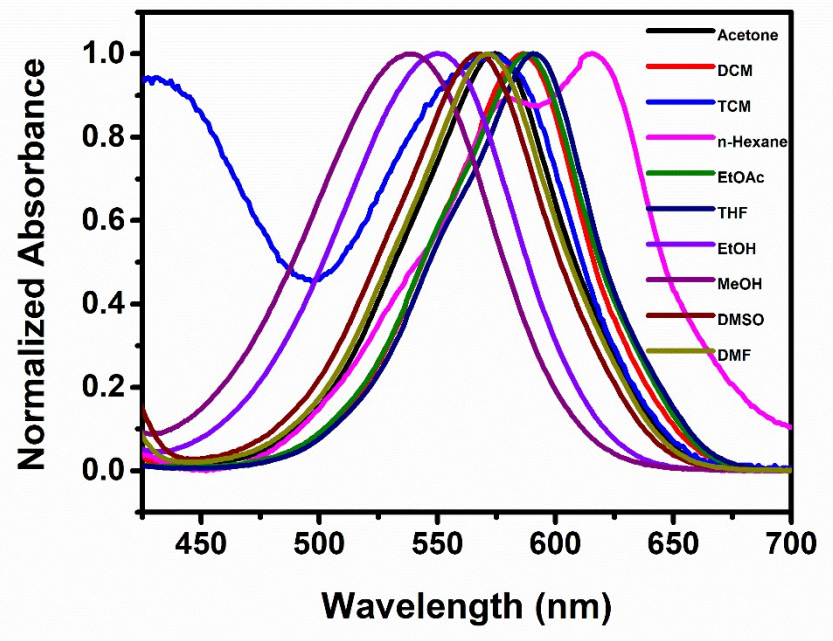

Fig. S10 Normalized UV-vis absorption spectra of **S1** upon irradiation with UV light for 1 min under different solvent conditions (concentration: 1×10^{-4} M).

The color of MC in methanol and ethanol is same as in PAN film (magenta). Overall, the absorption peaks are blue-shifted with the increase of solvent polarity. Therefore, the surrounding environment plays a crucial role in changing the charge distribution of MC.

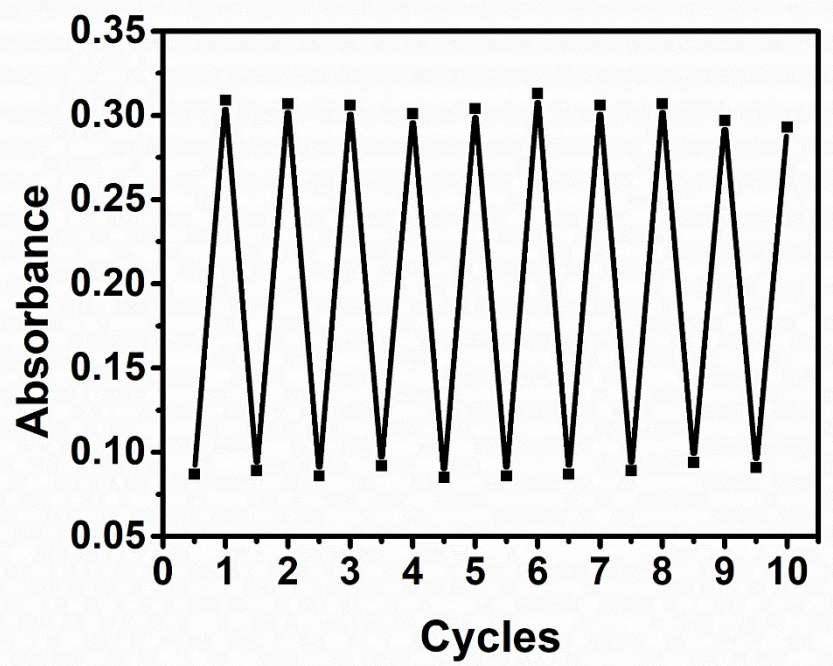

Fig. S11 Reversible switch of the absorption intensity of **S1** at 556 nm by alternating UV irradiation and heat treatment in PAN film.

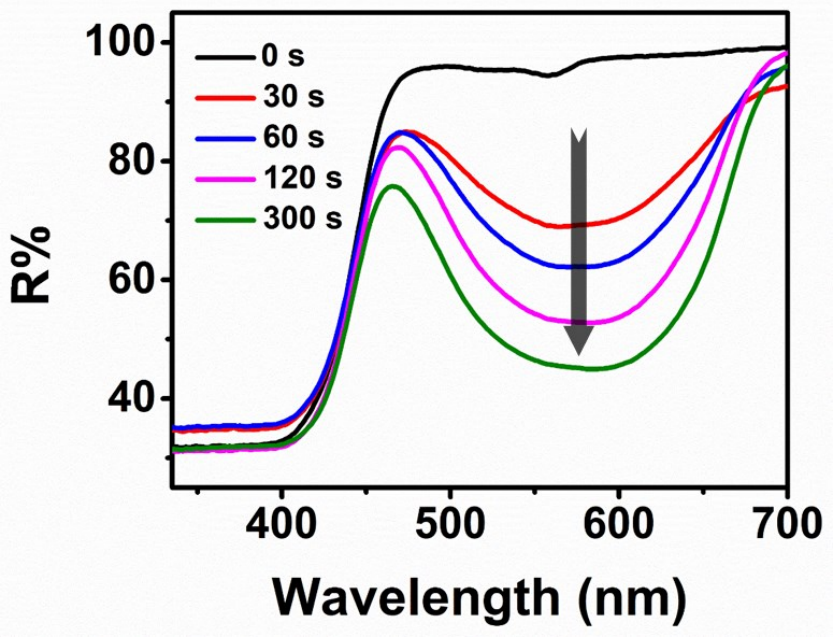

Fig. S12 Time-dependent diffuse reflectance spectra of **S1-I** with UV light irradiation.

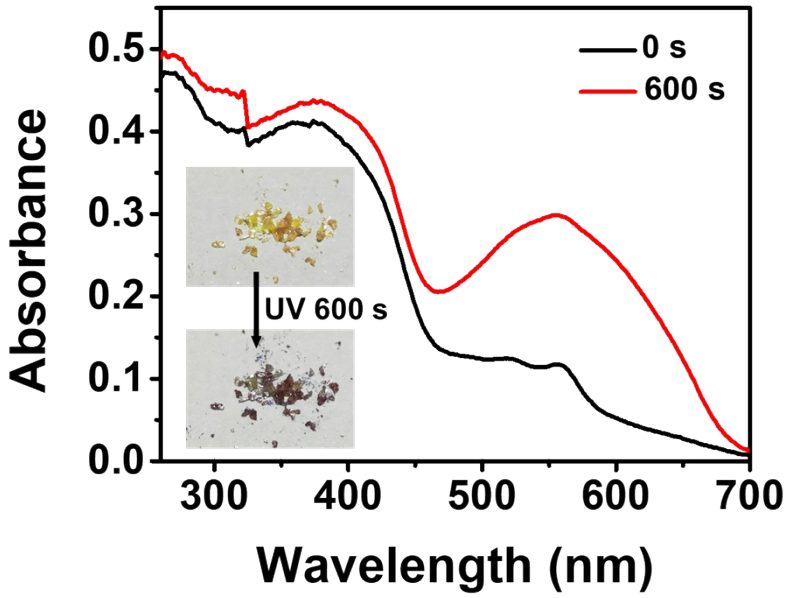

Fig. S13 UV-vis absorption spectra of **S1-C** before and after UV light irradiation. The insets are the reversible apparent color changes of **S1-C**.

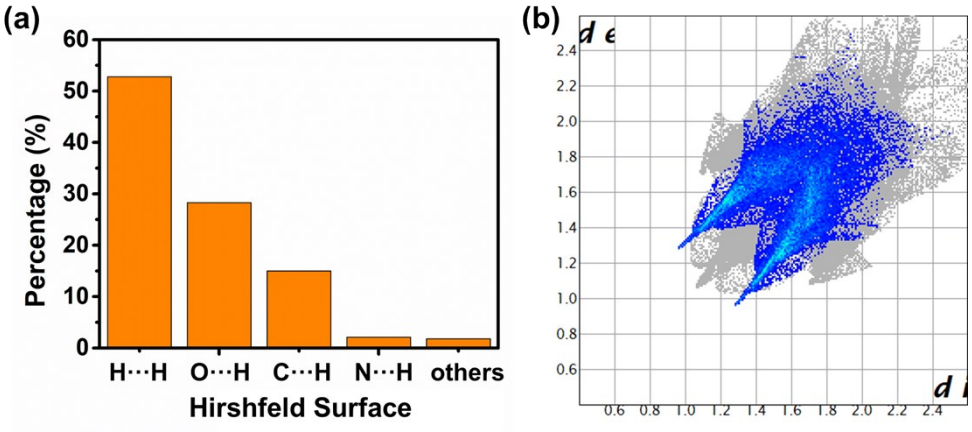

Fig. S14 (a) Individual atomic contact percentage contribution to the Hirshfeld surface in **S1-C**. (b) 2D fingerprint plot of H···O interactions in **S1-C**.

The red areas on the surfaces stand for the O···H interactions, exhibiting correlated spikes in the 2D fingerprint plots. While, there is no strong intermolecular interactions, such as π-π stacking and hydrogen bonding in **S1-C**, resulting in a relatively loose packing mode.

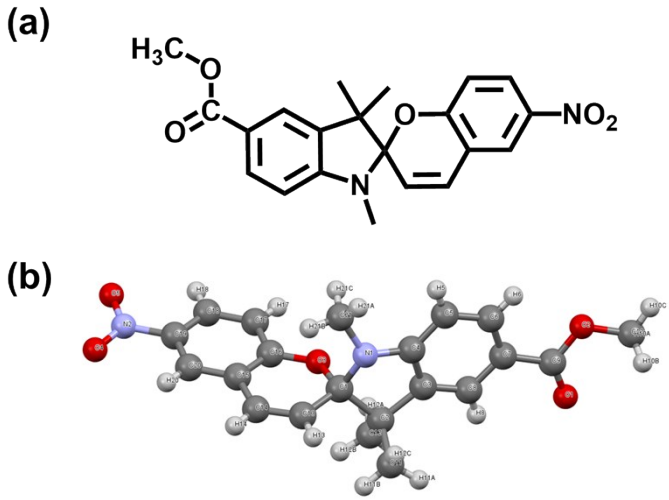

Fig. S15 (a) Chemical structure of compound **SP2**. (b) Molecular structure of **SP2** single crystal. **SP2** is the crystal structure (CCDC 1838532) we previously reported, which cannot show photochromism in the solid state.[1]

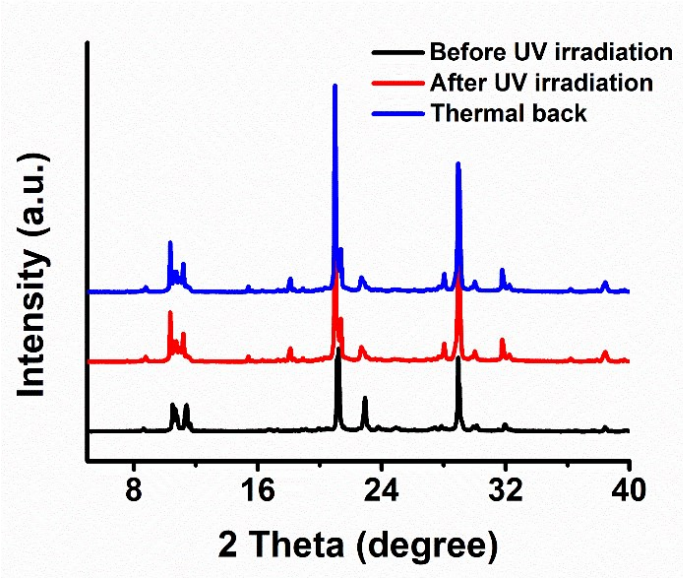

Fig. S16 PXRD patterns of **S1-C** under different conditions.

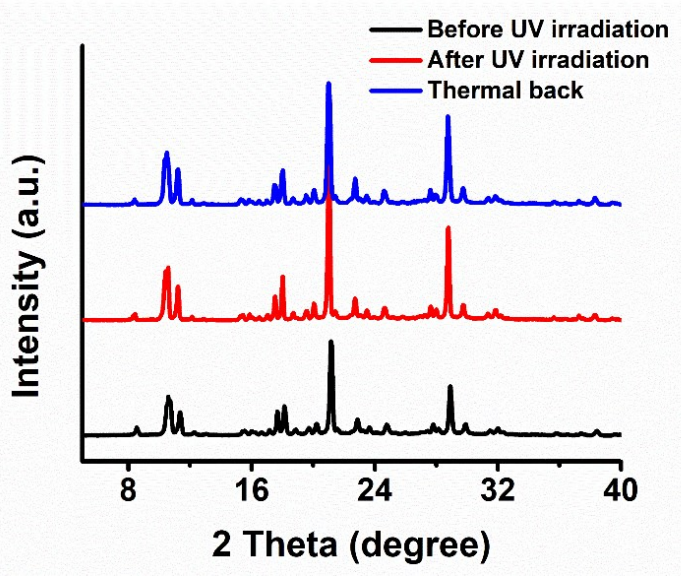

Fig. S17 PXRD patterns of **S1-I** under different conditions.

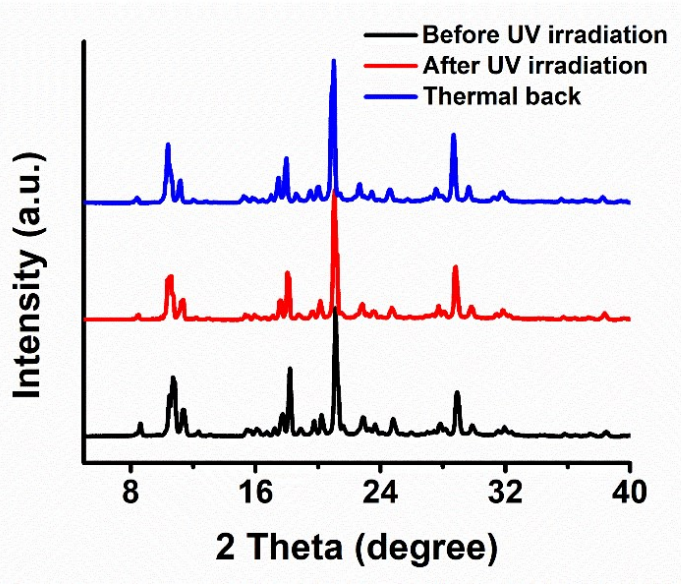

Fig. S18 PXRD patterns of **S1-G** under different conditions.

As shown in Fig. S16-18, the PXRD patterns were performed to study the packing modes of **S1-C**, **S1-I** and **S1-G** samples after irradiation and subsequent thermal back-isomerization. Although **S1-C**, **S1-I** and **S1-G** samples can all achieve photochromism after UV irradiation for 10 min, the PXRD patterns show little changes. Therefore, the packing modes of **S1-C**, **S1-I** and **S1-G** samples remain the same after UV irradiation.

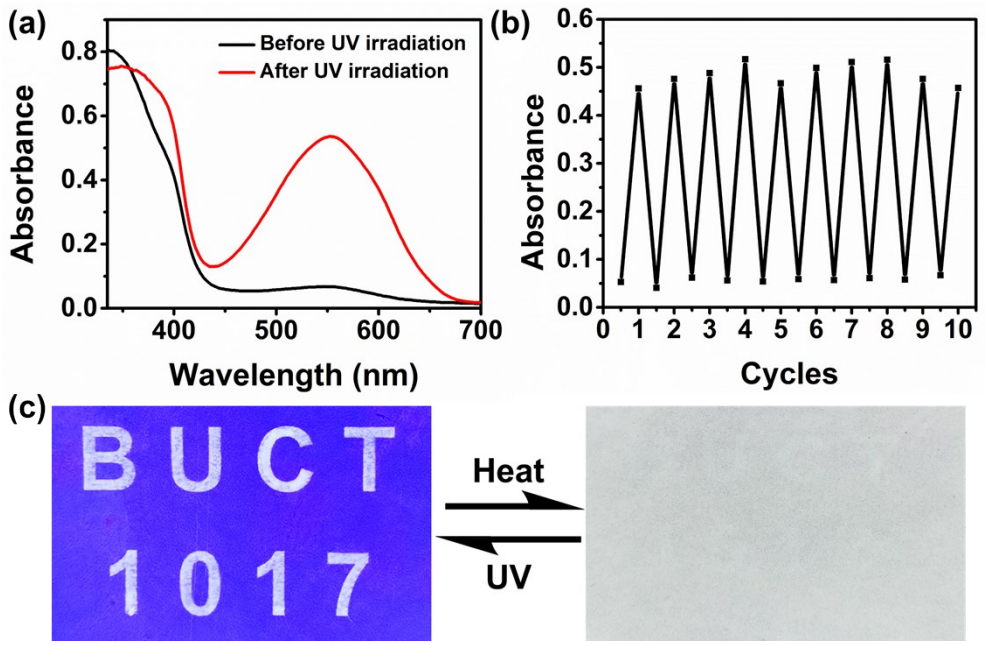

Fig. S19 (a) UV-vis absorption spectra of **S1** on the filter paper before and after UV light irradiation. (b) Reversible switch of the absorption intensity of **S1** at 583 nm by alternating UV irradiation and heat treatment. (c) Reversible optical printing under alternating UV and heat treatment.

The filter paper, treated by **S1** solution (0.2 mg/mL) and then dried, can be written with UV light through a photomask. As shown in Fig. S19, the area uncovered by the photomask on the filter paper shows blue color, and the covered part does not change color. Therefore, clear and distinct letters are obtained. To erase the written information, the filter paper can be handled with heat treatment (at about 70 ℃) for only 60 s, and then the filter paper was almost reverted to its original state.

Single crystal structure: The crystallographic information has been deposited with Cambridge Crystallographic Data Centre, and signed to CCDC codes 2042661 for **S1**. The detailed data are shown below.

Table S1. The detailed crystal data for **S1**.

Molecule	**S1**
Empirical formula	$C_{22}H_{22}N_2O_5$
Formula weight	394.42
Crystal system	monoclinic
Space group	$P2_1/n$
a / Å	9.5881(7)
b / Å	20.4736(10)
c / Å	10.6543(6)
α/°	90.00
β/°	111.067(7)
γ/°	90.00
Volume (Å^3)	1951.7(2)
Z	4
ρ_{calc}/mg mm^{-3}	1.342
F(000)	832
Reflections collected	9692
Independent reflections	3831[R(int) = 0.0313 (inf-0.9Å)]
Data/restraints/parameters	3831/0/265
Goodness-of-fit on F^2	1.052
Final R indexes [all data]	R_1 = 0.0628, wR_2 = 0.1047
Largest diff. peak/hole / e Å^{-3}	0.235/-0.259

References

1. Z. Wu, K. Pan, S. Mo, B. Wang, X. Zhao and M. Yin, *ACS Appl. Mater. Interfaces*, 2018, **10**, 30879-30886.